

Microscopic reaction diffusion patterns generated in nanometer size confinements

Jorge Carballido-Landeira* and Alberto P. Muñozuri

Universidad de Santiago de Compostela, Santiago de Compostela, Spain

*E-mail: jorge.carballido@gmail.com

Abstract: The Belousov-Zhabotinsky (BZ) reaction is one of the most studied reaction-diffusion systems able to display periodic oscillations when continued stirred and target patterns and/or spirals in spatially extended systems. Once the BZ reaction is placed inside nanometric micelles surrounded by an anionic surfactant and dispersed in an oleic system, the variety of spatial patterns increase considerably. The diversity on pattern formation is originated by the two different diffusion mechanisms available depending on the reagents charge nature. Non-polar chemicals may diffuse through the membrane and into the octane while polar chemicals diffuse within the entire nanodroplet, almost two orders of magnitude slower. On changing the confinement conditions where the BZ reaction takes place, the BZ-AOT system is able to present different dynamics, ranging from Turing structures (such as spots, stripes or labyrinthine) to standing waves, antispirals and packet waves.

Keywords: Reaction Diffusion systems. Belousov-Zhabotinsky reaction. Active microemulsion.

1. Introduction

The Belousov-Zhabotinsky (BZ) reaction is considered a prototype system for studies of reaction-diffusion phenomenon. This oscillatory chemical reaction involves the bromination and consequently oxidation of an organic substrate (originally citric acid) by bromate ions immersed into a strongly acidic solution [1]. Typically the catalysts used in the BZ reaction are cerium or ferroin, but the presence of ruthenium bipyridyl $[\text{Ru}(\text{bpy})_3^{+2}]$ complex has demonstrated photosensitive features in the BZ reaction. The presence of a redox indicator exhibiting different colors in the reduced and oxidized state of catalyst helps to visualize periodical temporal oscillations while the reaction is continuously stirred or spatiotemporal patterns when the reaction is kept unstirred [2].



The possibility to encapsulate the BZ reaction into nanodroplets of nanometric micelles bridges the gap between reaction diffusion systems and the effects of confinements. Thus, the BZ reagents are confined into nanometer-sized aqueous droplets surrounded by a surfactant monolayer and soaked in a continuous hydrophobic phase (octane). Here, the polar surfactant heads are orientated inwards (towards the droplet core), while the hydrophobic tails face the oil continuous phase [3].

There are two important parameters that define the reverse microemulsions. One of them is the hydrodynamic radius of the nanodroplets (R_d), which is defined as the addition of the size of the surfactant monolayer and the water nanodroplet core (R_w) [4]. The former is determined by the surfactant size (typically the anionic sodium bis(2-ethylhexyl) sulfosuccinate also known as AOT) and the latter is proportional to the molecular ratio between the aqueous and oil phase (ω_0):

$$R_w = 1.7\omega_0$$

The other main characteristic is the volume fraction of the water phase, defined as

$$\phi_w = \frac{V_w}{(V_w + V_o)}$$

where V_w and V_o are the volume of the aqueous and oil phases of the system of the micro-emulsion system. These properties of the micro-emulsion have a direct influence in the measurable features of the BZ reaction [5-7]

The so-called BZ-AOT system presents two different diffusive mechanisms of the chemical components. Polar BZ reagents are confined into the aqueous phase of the reverse microemulsion and diffuse with the water nanodroplets. The diffusion coefficient is then determined by the Stokes-Einstein equation:

$$D_d = \frac{K_B T}{6\pi\eta R_d}$$

where K_B , T , η are Boltzmann constant, the absolute temperature and the viscosity of the solvent, respectively.

In the course of the reaction several nonpolar intermediates are generated. These non-polar chemicals are able to diffuse through the membrane and into the oleic phase as single molecules with exhibiting diffusion coefficients almost two orders of magnitude faster than usual nanodroplets. Among the intermediates are the Br_2 and BrO_2 , which are known as fast-diffusing inhibitor and fast-diffusing activator, respectively [3].

2. The Model and Simulations

In order to model the main characteristics of the BZ-AOT system, Vanag and Epstein have proposed a variation of the well-known Oregonator model [8]. Thus, their model accounts those species able to migrate into the oleic phase in addition to the “ordinary” chemical reactions occurring in the aqueous compartments. The dynamics achieved in the BZ-AOT system can be expressed by the following set of differential equations [3]:

$$\frac{\partial x}{\partial \tau} = F(x, z, s, u) + D_x \Delta x \quad (1)$$

$$\frac{\partial z}{\partial \tau} = G(x, z, s, u) + D_z \Delta z \quad (2)$$

$$\frac{\partial s}{\partial \tau} = H(x, z, s, u) + D_s \Delta s \quad (3)$$

$$\frac{\partial u}{\partial \tau} = K(x, z, s, u) + D_u \Delta u \quad (4)$$

with

$$F(x, z, s, u) = -fz \frac{(x - q)}{(x + q)} + x(1 - \beta) - x^2 + s$$

$$G(x, z, s, u) = x - z(1 + \alpha) + \gamma u + D_z \Delta z$$

$$H(x, z, s, u) = \frac{1}{\varepsilon_1} (\beta x - s + \chi u) + D_s \Delta s$$

$$K(x, z, s, u) = \frac{1}{\varepsilon_2} (\alpha z - \gamma u) + D_u \Delta u$$

where x, z are the dimensionless concentrations of HBrO_2 and the catalyst of the reaction (i.e. ferriox, $\text{Ru}(\text{bpy})$, cerium), while s and u are the species soluble into the oleic phase: the inactive form of activator (BrO_2) and the inhibitor (Br_2), respectively. To account the differences in the diffusion rates we used $D_s = D_u \gg D_x = D_z$

The homogeneous steady state concentrations can be achieved by finding the solutions of the equations (1)-(4) once the temporal and spatial derivatives are setted to zero, *i.e.*, by solving $F(x, z, s, u) = 0$, $G(x, z, s, u) = 0$, $H(x, z, s, u) = 0$ and $K(x, z, s, u) = 0$. The stability of each one of the possible steady states will be determined by the eigenvalues obtained through the characteristic equation [9]:

$$\det(\mathbf{A} - \lambda \mathbf{I} - k^2 \mathbf{D}) = 0$$

where \mathbf{I} is the identity matrix, \mathbf{D} is the matrix of the diffusion coefficients here consider diagonal (neglecting cross-diffusion effects (even though they have been experimentally observed in the BZ-AOT systems) and \mathbf{A} is the Jacobian matrix of equations (5)-(6):

$$A(x, z, s, u) = \begin{pmatrix} \left(1 - \beta - 2x - \frac{f(q-x)z}{(q+x)^2} - \frac{fz}{(q+x)}\right) / \varepsilon & f(q-x) / \varepsilon(q+x) & 1/\varepsilon & 0 \\ 1 & -1 - \alpha & 0 & \gamma \\ (\beta \varepsilon_2) & 0 & -(1/\varepsilon_2) & \chi \varepsilon_2 \\ 0 & \alpha \varepsilon_3 & 0 & -\gamma \varepsilon_3 \end{pmatrix}$$

We observed that although Turing and Hopf instabilities may coexist in our range of parameters, the predominant mode differs according to the diffusion coefficient ratio (Figure 1). Thus, when the diffusion coefficient of the non-polar species is almost two-fold larger than the diffusion of the entire nanodroplet the dispersion relationship exhibits a predominant Turing mode slightly predisposed by Hopf domain (purple curve in Figure 1). However, decreasing the ratio of diffusion coefficients the Hopf mode prevails (red curve) until the Turing mode vanishes (black curve).

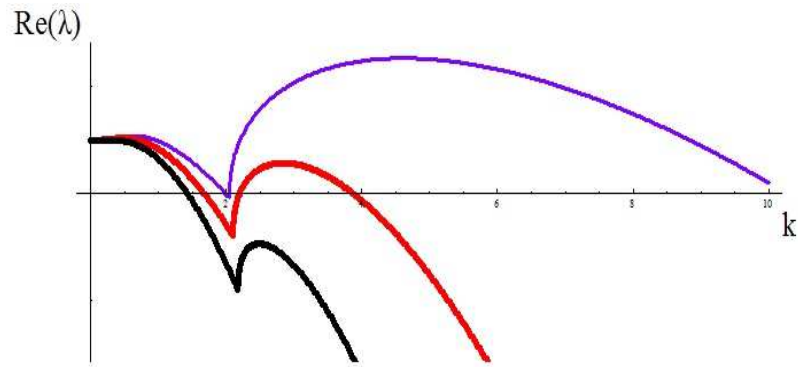


Figure 1. Dispersion relations exhibiting the interaction between the Turing and Hopf instabilities for different ratios between nonpolar intermediates and polar species confined in the microemulsion (D_s/D_x):80 (violet curve), 40 (red), 8 (black) . The model parameters to obtain this dispersion relations are $\alpha=8$;

$\beta=0.34$; $\gamma=0.2$; $\chi=0.$; $f=1.1$; $q=0.001$; $\varepsilon=0.37$; $\varepsilon_2=1.5$; $\varepsilon_3=0.006$;

Initially, we will consider the set of equations (1)-(4) in the absent of diffusion, *i.e.* without special considerations. This case resembles those reactions carried out under continuously stirring conditions in beakers. To do that, we use an Euler method with a time step of 0.01 time units (t.u.). Under these conditions, the BZ-AOT model exhibits an oscillatory solution with a characteristic period. Figure 2 (top) demonstrates this periodically behavior of the species concentration oscillating between a maximum and a minimum values.

Once diffusion was considered, simulations of equations (1)-(4) were performed by a Dufort-Frankel method in addition to Dirichlet and Newman conditions:

$$\begin{aligned} x(\bar{r}, t) \Big|_{t=t_0} &= x_{ini} \quad ; \quad \Big|_{\partial\Omega} \nabla x = 0 \\ z(\bar{r}, t) \Big|_{t=t_0} &= x_{ini} \quad ; \quad \Big|_{\partial\Omega} \nabla z = 0 \\ s(\bar{r}, t) \Big|_{t=t_0} &= s_{ini} \quad ; \quad \Big|_{\partial\Omega} \nabla s = 0 \\ u(\bar{r}, t) \Big|_{t=t_0} &= u_{ini} \quad ; \quad \Big|_{\partial\Omega} \nabla u = 0 \end{aligned}$$

Under Turing conditions (violet curve in Figure 1) we observed stationary patterns separated an equidistant wavelength. In Figure 2 (left panel) we show two characteristic Turing structures obtained by tuning the model parameters. The white (black) color in these figures stands for a high (low) concentration of the oxidized catalyst. Both kind of Turing patterns, spots and stripes, are experimentally achieved in the BZ-AOT system once the active micro-emulsion is sandwiched between two optical windows (Figure 2 right panel). The similitude between numerical and experimental patterns suggests that model (1)-(4) is a good candidate to display those structures obtained in the BZ-AOT system.

In addition to stationary Turing structures, the BZ-AOT system exhibits a rich variety of dynamics not possible without the confinement into nanodroplets, such as dashed waves, standing and packet waves, oscillons, segmented waves, etc [10-13]

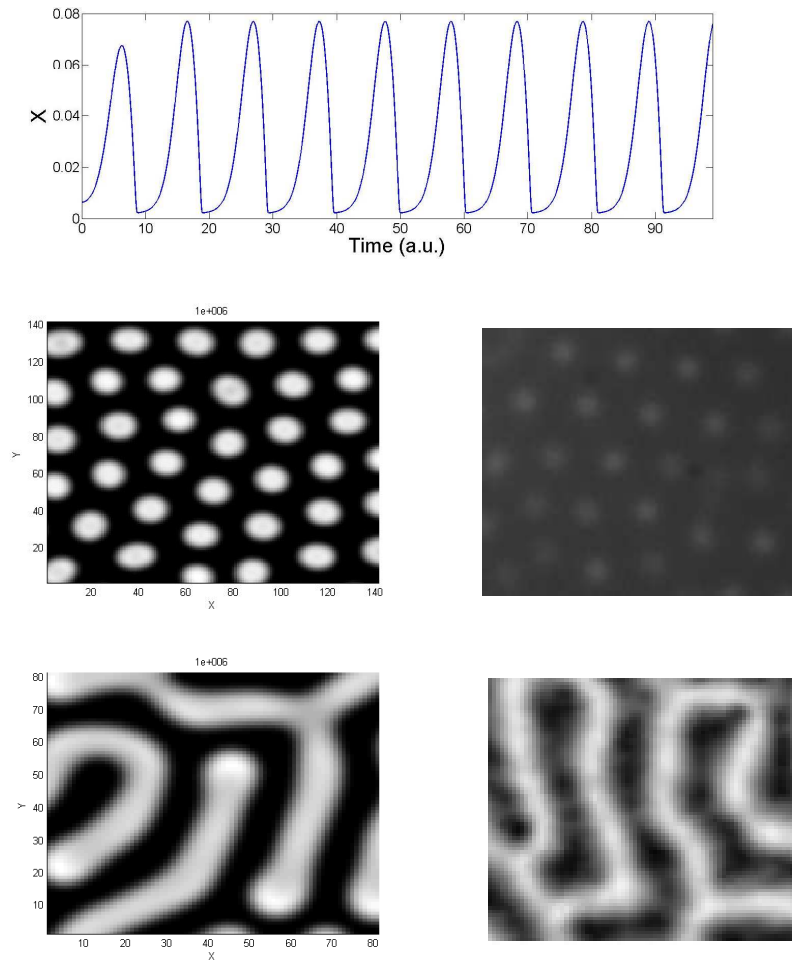


Figure 2. Model simulations of equations (1)-(4). Top: periodically temporal oscillations obtained in absence of diffusion. Middle and bottom: Two dimensional structures achieved numerically (left panel) and the comparative with experimental results (right panel) .

3. Conclusions

The confinement of a chemical oscillator into a micro-emulsion system generates a variety of spatial patterns not accessible without the compartmentalization. The diversity on pattern formation is understood by the presence of two different diffusion mechanisms. While Non-polar species may diffuse into the oleic phase, polar reagents are restricted to diffuse inside the nano-droplet system, being their diffusion coefficient considerably slower. The differences in the diffusion coefficients have been accounted by a four variable model, composed by two fast-diffusing species and two slow ones. We demonstrate the presence of Turing structures, which are patterns stationary in time with a characteristic spatial wavelength. Furthermore, we also present experimental results that qualitatively agree with our numerical simulations, validating our four variable model. It is remarkable to mention that there are several models to represent compartment active systems. They are have been indiscriminately used to characterize the arising of new dynamics as well as the influence of external forcing into the well-known patterns [14-18]. Recently, cross-diffusion of the chemical reactants was considered one of the probable mechanisms to achieve such diversity of pattern formation and has been added to the model scheme [19].

References

1. B. P. Belousov, *Collected Abstracts on Radiation Medicine*. Moscow: Medgiz: A. V. Lebedinskii. Page 145 (1959.)
2. A.N. Zaikin, and A. M. Zhabotinsky, *Nature (London)*, 225, 535. (1970)
3. V. K. Vanag, *Phys.-Usp.*, 2004, 47, 923–941.
4. A.M. Cazabat, D. Langevin, D. and D.Pouchelon, *J. Colloid Interface Sci.*, 73, 1. (1980)
5. V.K. Vanag, and D.V. Boulanov, *JPhys. Chem.*, 1998, 1449 (1994)
6. E. Villar-Alvarez, *et al.* *The Journal of Chemical Physics*, 134 094512 (2011)
7. J. Carballido-Landeira, P. Taboada and A. P. Muñuzuri, *Phys. Chem. Chem. Phys.*, 13, 4596, (2011)
8. R.J. Field, and R.M. Noyes, *J. Chem. Phys.*, 60, 1877 (1974)
9. Strogatz, S. 1994. *Nonlinear Dynamics and Chaos*. Massachusetts: Perseus Books.
10. V. K. Vanag and I. R. Epstein, *Phys. Rev. Lett.* **87**, 228301 (2001).
11. *J. Carballido-Landeira et al.* , *Phys. Chem. Chem. Phys.*, 10, 1094-1096, (2008)
12. V. K. Vanag and I. R. Epstein, *Phys. Rev. Lett.* **88**, 088303 (2002).
13. V. K. Vanag and I. R. Epstein *Phys. Rev. Lett* 92, 128301 (2004)
14. J. Guiu-Souto *et al.* , *Phys. Rev. E*, 82, 066209, (2010)
15. J. Carballido-Landeira, V. K. Vanag and I. R. Epstein, *Phys. Chem. Chem. Phys.*, 12, 3656-3665, (2010)

16. A. Kaminaga, V.K. Vanag, and I.R. Epstein. *Angew. Chem. Int. Ed.*, 118, 3159–3161. (2006)
17. J. Guiu-Souto *et al.*, *Soft Matter*, DOI: [10.1039/c3sm27624d](https://doi.org/10.1039/c3sm27624d) (2013)
18. J. Carballido-Landeira, P. Taboada and A. P. Munuzuri, *Soft Matter*, 8, 2945 (2012)
- V. K. Vanag, F. Rossi, A. Cherkashin, and I. R. Epstein, *J. Phys. Chem. B* **112**(30), 9058 (2008)